Reconstructing Polygons from Moments with Connections to Array Processing *

Peyman Milanfar
(Corresponding Author)
Alphatech Inc.,
50 Mall Road, Burlington, MA 01803
Phone: (617) 273-3388 extension 271
FAX: (617) 273-9345 E-mail: milanfar@alphatech.com

George C. Verghese,   W. Clem Karl,   Alan S. Willsky
Center for Intelligent Control Systems, and
Laboratory for Information and Decision Systems
Department of Electrical Engineering and Computer Science
Massachusetts Institute of Technology
Cambridge, Massachusetts, 02139

EDICS Number SP 3 and SP 2.5.1

January 10, 1994

Abstract

In this paper we establish a set of results showing that the vertices of any simply-connected planar polygonal region can be reconstructed from a finite number of its complex moments. These results find applications in a variety of apparently disparate areas such as computerized tomography and inverse potential theory, where in the former it is of interest to estimate the shape of an object from a finite number of its projections; while in the latter, the objective is to extract the shape of a gravitating body from measurements of its exterior logarithmic potentials at a finite number of points. We show that the problem of polygonal vertex reconstruction from moments can in fact be posed as an array processing problem, and taking advantage of this relationship, we derive and illustrate several new algorithms for the reconstruction of the vertices of simply-connected polygons from moments.

1 Introduction

In this paper we present novel algorithms for the reconstruction of binary polygons from their estimated *complex* moments. We show, in fact, that this problem can be formulated as an *array processing* [27] problem. The applications of the algorithms we develop to tomography hence expose a seemingly deep connection between the fields of tomography and array processing. This connection implies that a host of numerical algorithms such as MUSIC [28], Min-norm [18], and Prony [24] are now available for application to tomographic reconstruction problems.

Our algorithms are based on the idea that the vertices of a simply-connected polygonal region in the plane are determined by a finite number of its moments. Davis [5] showed, using the Motzkin-Schoenberg (MS) formula [29], that a triangle in the plane is uniquely determined by its moments of up to order 3. In the process of proving this result, Davis generalized the MS formula to arbitrary n-gons, and in this paper we make use of this result to generalize Davis' triangle result to arbitrary simply-connected polygons. In particular, we have generalized his result using Prony's method [13] to show that the vertices of a simply-connected, n-gon are uniquely determined by its complex moments of up to order $2n - 1$. We show that in tomographic terms, this implies that $2n - 2$ projections from distinct angles suffice to uniquely determine the vertices of any simply-connected n-gon. This result is an improvement on theoretical results dealing with reconstructability from few projections such as in [16, 19, 17, 7, 8, 9].

In Section 2, we discuss the mathematical basis of reconstruction of polygonal regions from a finite number of complex moments, and in Section 3 we make explicit connection to and use of Prony's method. In Section 3.1 we present some remarks regarding the reconstructability of the interior of polygons from their moments and briefly point out a connection to inverse potential theory. In Section 4, we discuss the explicit connection of the polygonal reconstruction problem to algorithms in array processing and present

several reconstruction algorithms, and in Section 5 we discuss a novel application of the ideas describe in this paper to the problem of tomographic reconstruction of polygons, and illustrate our method with examples of polygonal reconstruction from tomographic data. Finally, Section 6 contains our conclusions.

2 Mathematical Background

In 1977 Davis [5] showed that any triangular region in the plane is uniquely determined by its first four complex moments. This results was derived as a corollary to a little known result which he termed the *Motzkin-Schoenberg Formula*. He had worked out an alternative proof of this formula in an earlier (1964) paper [6], where he also generalized this formula to the case of n-sided polygons. As we prove in the next section, this generalized formula can, in fact, be used to generalize Davis' result for triangles. In particular, we show that the vertices of n-sided, simply-connected polygonal regions in the plane are uniquely determined by a finite number of their complex moments. As we will see, this result, which had eluded Davis, is easily proven by transforming this problem into one to which Prony's method can be applied.

Let T denote a triangle in the complex plane whose vertices are given by z_1, z_2, and z_3. If A denotes the area of T and $h(z)$ is *any* analytic function in the closure of T, the **Motzkin-Schoenberg (MS) Formula** [29, 6, 5] states that

$$\int\int_T h''(z)\, dx\, dy = 2A \det(U)/\det(V) \tag{1}$$

where

$$U = \begin{bmatrix} 1 & 1 & 1 \\ z_1 & z_2 & z_3 \\ h(z_1) & h(z_2) & h(z_3) \end{bmatrix} \tag{2}$$

3

$$V = \begin{bmatrix} 1 & 1 & 1 \\ z_1 & z_2 & z_3 \\ z_1^2 & z_2^2 & z_3^2 \end{bmatrix} \tag{3}$$

By considering triangulations of such n-gons, Davis [6] extended this formula to show that the value of the integral of the second derivative of *any* analytic function in the closure of a polygonal region of the complex plane depends *only* on the values of this function at the vertices of the polygonal region in question:

Theorem 1 *[6] Let z_1, z_2, $\cdots$, z_n designate the vertices of a polygon P. Then we can find constants a_1, $\cdots$, a_n depending upon z_1, z_2, $\cdots$, z_n, (and the way they are connected) but independent of h, such that for all h analytic in the closure of P,*

$$\int\int_P h''(z)\, dx\, dy = \sum_{j=1}^{n} a_j h(z_j). \tag{4}$$

If $r \geq n$ and z_{n+1}, $\cdots$, z_r are additional points distinct from z_1, $\cdots$, z_n, and if there are constants b_1, $\cdots$, b_r which depend only upon z_1, $\cdots$, z_r such that

$$\int\int_P h''(z)dx dy = \sum_{j=1}^{r} b_j h(z_j) \tag{5}$$

for all h analytic in the closure of P, then

$$b_j = a_j, \quad 1 \leq j \leq n \tag{6}$$

$$b_j = 0, \quad n + 1 \leq j \leq r \tag{7}$$

Two observations are in order about the implications of this result. First, we can prove the following result for simply connected polygons using the same line of reasoning as Davis [6].

Lemma 1 *Let P be a simply-connected polygonal region. The coefficients $\{a_j\}$ in (4) are all nonzero if and only if P is nondegenerate.*

Proof: Using Green's theorem in the complex plane and the Cauchy-Riemann equations for analytic functions [4, 6], the integral in (4) can be rewritten as

$$\int\int_P h''(z)\, dx\, dy = \frac{i}{2}\int_{\partial P} h'(z)\, d\bar{z} \tag{8}$$

where $i = \sqrt{-1}$, ∂P denotes the boundary of P, and $\bar{z}$ denotes the complex conjugate of z. The assumption that P is simply connected implies that the boundary of P consists of n straight lines which we call s_1, s_2, $\cdots$, s_n; where s_j connects the vertices z_j and z_{j+1}. (For convenience, we assume that the vertices z_j of P are arranged in the counter-clockwise direction in the order of increasing index, and that $z_{n+1} = z_n$). Hence, splitting the right-hand side of (8) into a sum of terms over the sides and using the expression for the equation of a line in the complex plane [6, 4], we can write

$$\int\int_P h''(z)\, dx\, dy = \frac{i}{2}\sum_{j=1}^n (\alpha_{j-1} - \alpha_j)h(z_j) \tag{9}$$

where

$$\alpha_j = \frac{\bar{z}_j - \bar{z}_{j+1}}{z_j - z_{j+1}}. \tag{10}$$

With some algebraic manipulation, it is not difficult to show that

$$\frac{i}{2}(\alpha_{j-1} - \alpha_j) = \frac{2A_j}{(z_j - z_{j+1})(z_j - z_{j-1})} \tag{11}$$

where A_j is the signed area of the triangle formed by the vertices z_{j-1}, z_j, and z_{j+1} given by

$$A_j = \frac{i}{4}\det\begin{bmatrix} z_{j-1} & \bar{z}_{j-1} & 1 \\ z_j & \bar{z}_j & 1 \\ z_{j+1} & \bar{z}_{j+1} & 1 \end{bmatrix} \tag{12}$$

Now comparing (9) to (4), and using (11) we see that

$$a_j = \frac{i}{2}\left(\frac{\bar{z}_{j-1} - \bar{z}_j}{z_{j-1} - z_j} - \frac{\bar{z}_j - \bar{z}_{j+1}}{z_j - z_{j+1}}\right) = \frac{2A_j}{(z_j - z_{j+1})(z_j - z_{j-1})}, \qquad j = 1, \cdots, n \tag{13}$$

Hence, no a_j is zero unless the corresponding A_j is zero. This can occur if and only if P is degenerate. i.e. for some j, the triangle formed by z_{j-1}, z_j, and z_{j+1} is degenerate. $\qquad\square$

Note that (13) is an expression that depends explicitly on the vertices *and* on the order in which these

vertices are connected since (13) requires that we explicitly order the z_j. If we limit ourselves to convex objects, then there is in essence a unique ordering of the vertices except for an inconsequential cyclic permutation. However, as we discuss further in Section 3.1, in general there may be several nontrivially distinct ways in which the vertices may be connected in order to form simply-connected polygons, and (13) depends on the specific choice of ordering corresponding to the polygon P.

A second observation is that the formula (4) is a *minimal* representation of the integral of h'' over P in terms of discrete values of h. Specifically, the left-hand side of (4) depends *only* on the values of h at the vertices of P and how they are connected; what values h takes at other points in the complex plane are completely irrelevant in this regard. Furthermore, since each of the a_j is nonzero, the representation (4) for arbitrary $h(z)$'s can not be reduced to one involving $h(z)$ at fewer points.

With these results as a foundation, we now develop the connection between complex moments and vertices. To begin, define the geometric moments of an function f over a compact domain $\mathcal{O}$ as

$$\mu_{pq} = \iint_{\mathcal{O}} f(x,y) x^p y^q \, dx \, dy. \tag{14}$$

Let us also define the *simple complex moments* (**s-complex moments**) as [1]

$$c_k = \iint_{\mathcal{O}} f(x,y) \, z^k \, dx \, dy \tag{15}$$

where $z = x + iy$. The relationship between the s-complex and geometric moments is simply established by expanding $(x + iy)^k$:

$$c_k = u_k^T \mu^{(k)} \tag{16}$$

where

$$u_k = \left[\begin{pmatrix} k \\ 0 \end{pmatrix} i^0, \cdots, \begin{pmatrix} k \\ k \end{pmatrix} i^k \right]^T, \quad \mu^{(k)} = [\mu_{k0} | \mu_{k-1,1} | \cdots | \mu_{1,k-1} | \mu_{0,k}]^T \tag{17}$$

Now consider Theorem 1 and let (I) $h(z) = z^k$ and (II) $f(x,y)$ be the indicator function over a

---

[1] These moments are also referred to as *harmonic* moments in the mathematics literature.

simply-connected polygonal region P of the plane. Then, this theorem states that for any nondegenerate, simply-connected, n-gon P in the plane, we have

$$\int\int_P (z^k)'' \, dx \, dy = \sum_{j=1}^n a_j z_j^k.$$ (18)

where the a_j are as defined in (13). The left hand side of this identity can be written as

$$\int\int_P (z^k)'' \, dx \, dy = k(k-1)\int\int_P z^{k-2} \, dx \, dy = k(k-1)c_{k-2}.$$ (19)

Defining the numbers $\tau_k = k(k-1)c_{k-2}$, which we term *weighted complex moments* (**w-complex moments**), with $\tau_0 = \tau_1 = 0$, we have

$$\tau_k = \sum_{j=1}^n a_j z_j^k.$$ (20)

Equation (20) is, for every k, a direct relationship between the w-complex moments and the vertices of P. We next show that the vertices of P may be uniquely recovered from knowledge of a sufficient number of the τ_k.

3 Vertices from Complex Moments via Prony's Method

Assume that the n-gon P is simply-connected and nondegenerate, and let us consider Equation (20) for $k = 0, 1, \cdots, 2n - 1$. Written in vector form we have

$$\begin{bmatrix} \tau_0 \\ \tau_1 \\ \vdots \\ \tau_{2n-1} \end{bmatrix} = \begin{bmatrix} 1 & 1 & \cdots & 1 \\ z_1 & z_2 & \cdots & z_n \\ \vdots & \vdots & \ddots & \vdots \\ z_1^{2n-1} & z_2^{2n-1} & \cdots & z_n^{2n-1} \end{bmatrix} \begin{bmatrix} a_1 \\ a_2 \\ \vdots \\ a_n \end{bmatrix}$$ (21)

$$\mathcal{T}_{2n} \equiv \mathcal{V}_{2n} \mathbf{a}_n$$ (22)

where the obvious associations have been made in the last identity. We will use Prony's method [13] here to show that the vertices $\{z_j\}$ can be computed from the w-complex moment vector $\mathcal{T}_{2n}$ given by Equation (22). Davis [5] showed this result for $n = 3$ (the triangular case) using algebraic manipulations. By

7

identifying and exploiting the relationship of the moment-to-vertices problem with very similar problems in signal and array processing we directly obtain both the generalization of this result using Prony's method as well as a number of algorithms for the solution of the problem.

Define the polynomial $P(z)$ as

$$P(z) = \prod_{j=1}^{n}(z - z_j) = z^n + \sum_{j=1}^{n} p_j z^{n-j}, \tag{23}$$

and consider its associated coefficient vector $p^{(n)} = [p_n, p_{n-1}, \cdots, p_1]^T$. We show that the coefficients of $P(z)$ can be uniquely determined from $\mathcal{T}_{2n}$. To this end, form the $2n \times 2n$ matrix K_{2n} from $p^{(n)}$ as follows

$$K_{2n} = \begin{bmatrix} p_n & \cdots & p_1 & 1 & & \bigcirc \\ & \ddots & & \ddots & \ddots & \\ \bigcirc & & p_n & \cdots & p_1 & 1 \end{bmatrix}. \tag{24}$$

We now proceed as in Prony's method [13]. Specifically, from the definition of $P(z)$ it follows that

$$K_{2n}\mathcal{T}_{2n} = K_{2n}\mathcal{V}_{2n}\mathbf{a}_n = \underline{0} \tag{25}$$

The identity $K_{2n}\mathcal{T}_{2n} = \underline{0}$ can be rewritten as

$$\begin{bmatrix} \tau_0 & \tau_1 & \cdots & \tau_{n-1} \\ \tau_1 & \tau_2 & \cdots & \tau_n \\ \vdots & \vdots & \ddots & \vdots \\ \tau_{n-1} & \tau_n & \cdots & \tau_{2n-2} \end{bmatrix} p^{(n)} = - \begin{bmatrix} \tau_n \\ \tau_{n+1} \\ \vdots \\ \tau_{2n-1} \end{bmatrix} \tag{26}$$

$$H_n p^{(n)} = -h_n \tag{27}$$

To show that we can uniquely recover $p^{(n)}$ from this last identity, we must now show that H_n is invertible.

Lemma 2 *The $n \times n$ matrix H_n is invertible if and only if the corresponding simply-connected polygon P is a nondegenerate n-gon.*

Proof: The result is arrived at by noticing that H_n can be decomposed as

$$H_n = \mathcal{V}_n diag(\mathbf{a}_n)\mathcal{V}_n^T \tag{28}$$

8

where $\mathcal{V}_n$ is the *Vandermonde* matrix of the vertices $\{z_j\}$ defined as follows

$$\mathcal{V}_n = \begin{bmatrix} 1 & 1 & \cdots & 1 \\ z_1 & z_2 & \cdots & z_n \\ \vdots & \vdots & \ddots & \vdots \\ z_1^{n-1} & z_2^{n-1} & \cdots & z_n^{n-1} \end{bmatrix} \tag{29}$$

The matrix $\mathcal{V}_n$ has determinant

$$\det(\mathcal{V}_n) = \prod_{i>j}(z_i - z_j) \tag{30}$$

which vanishes if and only if P is degenerate. Furthermore, as a consequence of Lemma 1, the elements of

the vector $\mathbf{a}_n$ are all nonzero unless P is degenerate. Hence this Lemma is established. $\qquad\square$

As a consequence of this lemma, the coefficients of $P(z)$ can then be uniquely determined through

$$p^{(n)} = -H_n^{-1}h_n. \tag{31}$$

Given these coefficients, upon solving the polynomial equation $P(z) = 0$, the vertices of P may be recovered.

In summary, we have shown the following result.

Proposition 1 *Let P denote a nondegenerate, simply-connected, n-sided polygonal region in the plane.*

The vertices of P are uniquely determined by its w-complex moments τ_k up through order $2n - 1$.

Several useful corollaries follow from Proposition 1. Recall that the w-complex moments τ_k are related

to the s-complex moments c_k as $\tau_k = k(k - 1)c_{k-2}$. Hence, we have:

Corollary 1 *The vertices of a nondegenerate, simply-connected n-gon P in the plane are uniquely deter-*

mined by its s-complex moments of up to order $2n - 3$. i.e. c_k, $k = 0, 1, \cdots, 2n - 3$.

Also from (16) it follows that

Corollary 2 *The vertices of a nondegenerate, simply-connected n-gon P in the plane are determined by*

its geometric moments of up to order $2n - 3$. i.e. $\mu^{(k)}$, $k = 0, 1, \cdots, 2n - 3$.

9

3.1 Remarks

Proposition 1 and its corollaries imply that the vertices of P can be extracted from a finite number of moments. This result, however, does not tell us what the interior of P looks like. According to Proposition 1, from the set of moments we can decipher the locations of the vertices of P. Furthermore, from (22) we can also determine the coefficients $a_1, \cdots, a_n$ (this follows since the upper n rows of $\mathcal{V}_{2n}$ form the invertible matrix $\mathcal{V}_n$). Thus, according to Theorem 1, we can evaluate

$$\int\int_P h''(z)\, dx\, dy = \sum_{j=1}^n a_j h(z_j). \tag{32}$$

for *any* analytic function $h(z)$, including z^k for *any* nonnegative integer k. Hence, from knowledge of τ_1, $\cdots, \tau_{2n-1}$, we can determine *all* of the w-complex moments of P. Nevertheless, it is a remarkable fact that this information is *not* sufficient to uniquely specify P in general. In particular, a somewhat more general problem was formally posed in 1975 by H. Shapiro in [2]: "Let D_1 and D_2 be simply-connected compact sets such that

$$\int\int_{D_1} z^k\, dx\, dy = \int\int_{D_2} z^k\, dx\, dy \quad k = 0, 1, 2, \cdots \tag{33}$$

Must we have $D_1 = D_2$?" The answer is yes if the intersection of the closures of D_1 and D_2 is empty or consists of only one point, but in general the answers is, in fact, negative. In 1978, a counter-example to the general case was provided by M. Sakai in [26] where he constructed simple domains bound by a finite number of piecewise circular arcs. Polygonal counter-examples were later constructed by A. M. Gabrielov, V. N. Strakhov, and M. A. Brodsky and were published in the latter two authors' paper [30]. These authors arrived at this question from considering the more general problem of uniqueness of the shape and density of plane gravitating bodies as determined from their exterior logarithmic potential. A good survey of this problem from the point of view of inverse potential theory can be found in [31] [2].

---

[2]The authors would like to thank Chris Bishop of SUNY Stony Brook Math dept. and Prof. Pavel Etingof of Yale Math dept. for pointing out these references.

In certain special cases, however, the w-complex moments do uniquely specify the underlying polygon. For example, if the z_j form the set of vertices of a convex object, then there is obviously a unique way in which the z_j can be connected in order to delineate a simply-connected polygon. For nonconvex P, however, the situation is more complex, since as illustrated in Figure 1 for 4-sided figures, there is more than one way to connect the vertices. However, there are only a finite number of such possibilities that lead to distinct, simply-connected polygons. The question, then, is whether the finite number of distinct simply-connected polygons with vertices $z_1, \cdots, z_n$ can be uniquely distinguished from the knowledge of $a_1, \cdots, a_n$. As shown in [30], this is *not* the case in general, but as we now show, *is* true for large classes of nonconvex objects including those in Figure 1. In particular, we have the following:

Proposition 2 *Consider n distinct points $z_1, z_2, \cdots, z_n$ in the complex plane. Let P and P' be simply-connected, nondegenerate, n-gons generated by connecting these vertices in two distinct ways. If P and P' have at least one side in common, then for some $1 \leq j \leq n$,*

$$a_j(P) \neq a_j(P'), \tag{34}$$

where $a_j(P)$ and $a_j(P')$ are respectively defined by

$$\iint_P h''(z)dxdy = \sum_{j=1}^{n} a_j(P)h(z_j) \tag{35}$$

$$\iint_{P'} h''(z)dxdy = \sum_{j=1}^{n} a_j(P')h(z_j) \tag{36}$$

with h denoting any analytic function in the closure of $P \bigcup P'$.

Proof: We prove this result by contradiction. Assume that P and P' have at least one side in common. Without loss of generality, let us say this is the side give by connecting the vertices z_j and z_{j+1} of P for some $1 \leq j \leq n$. Now if $a_j(P) = a_j(P')$, it follows from (13) that

$$\frac{i}{2}\left(\frac{\overline{z}_{j-1} - \overline{z}_j}{z_{j-1} - z_j} - \frac{\overline{z}_j - \overline{z}_{j+1}}{z_j - z_{j+1}}\right) = \frac{i}{2}\left(\frac{\overline{z'}_{j-1} - \overline{z}_j}{z'_{j-1} - z_j} - \frac{\overline{z}_j - \overline{z}_{j+1}}{z_j - z_{j+1}}\right) \tag{37}$$

where z'_{j-1} is the $j - 1^{th}$ vertex of P'. Simplifying (37) yields

$$\frac{\overline{z}_{j-1} - \overline{z}_j}{z_{j-1} - z_j} = \frac{\overline{z'}_{j-1} - \overline{z}_j}{z'_{j-1} - z_j} \tag{38}$$

It is easy to check that this last expression (38) implies that the vertices z_j, z_{j-1}, and z'_{j-1} must be collinear. This is a contradiction to the assumption that P and P' are both nondegenerate. □

Note, for example, that in the case of 4-sided nonconvex figures as in Figure 1, there are only 3 distinct polygons with the given set of vertices, and each pair of these has a side in common. Thus, in this case we deduce that knowledge of $\tau_0, \cdots, \tau_7$, which uniquely determine $z_1, \cdots, z_4$, and $a_1, \cdots, a_4$, also uniquely specifies the polygon P. Furthermore, as the example in [30] shows, the cases in which nonuniqueness arise are extremely complex[3]. Indeed, as Proposition 2 makes clear, the only case in which this *might* happen is if two simply-connected polygons with the same vertices $z_1, \cdots, z_n$, have *no* edge in common. Thus for our purposes we assume that $z_1, \cdots, z_n$ define a finite set of possible polygons with distinct sets of coefficients $a_1, \cdots, a_n$.

4 Connections to Array Processing

Array processing has been a very active field of research in the past 2 decades motivated by applications in sonar, radar, oceanography, seismology, and speech processing, to name a few. The data to be analyzed in a standard array processing application [27, 25] consist of a sum of complex exponentials in additive white noise. This formulation corresponds to the problem of localizing several radiating sources by observation of their signals at spatially separated sensors. More formally, the general problem is that of estimating the unknowns b_j and z_j from the measured signals y_k given as follows

---

[3]In fact, the simply-connected nonconvex object with the smallest number of sides not uniquely determined by z_j and a_j has 22 sides [30]

$$y_k = \sum_{j=1}^{n} b_j z_j^k + v_k, \qquad k = 0, \cdots, N - 1 \tag{39}$$

Here, z_j denotes an unknown source, b_j denotes an unknown complex amplitude, and v_k denotes (complex) white noise. In standard array processing problems, the sources z_j are complex exponentials of the form $\exp(-i\phi_j)$, but general formulations where z_j is not restricted to this form have also been studied [14, 27].

Now assume that noisy estimates $\hat{\tau}_k$ of the w-complex moments of a simply-connected n-gon are given:

$$\hat{\tau}_k = \sum_{j=1}^{n} a_j z_j^k + w_k. \tag{40}$$

By comparing this measurement equation to (39), we can see that they have exactly the same form; whereby a vertex of the polygon can be interpreted as a radiating source whose corresponding (complex) amplitude shows how it is connected to the other vertices of the polygon. The general formulation of the array processing problem is therefore nearly the same as the formulation of the reconstruction problem of binary polygonal objects from noisy measurements of their w-complex moments. The main difference is that the coefficients a_j are *not* independent variables but are, in fact, deterministic functions of z_j and the order in which they are connected. Nevertheless, if we treat the a_j as independent unknowns, we *can* directly apply array processing methods and then check to see if the a_j so-determined are in fact consistent with one of the finite number of polygons with vertices given by the extracted values z_j.

In the remainder of this section we discuss the direct application of some array processing algorithms to the polygon reconstruction problem from moments. An exhaustive study of all available algorithms and their relative performance is beyond the scope of this paper and therefore, we present only one such general approach and some of its variants to illustrate the main concepts. The algorithms we consider are directly based on a generalization of Prony's method. In this context, we discuss the ordinary least squares Prony (OLSP), the total least squares Prony (TLSP), and the weighted least squares Prony (WLSP) techniques.

4.1 Least Squares Prony Techniques

We wish to estimate the parameters a_j and the vertices z_j corresponding to an n-sided polygonal region from noisy estimates of the first N ($\geq 2n$) w-complex moments of P. i.e. (40) for $k = 0, \cdots, N-1$, where we assume that w_k are (complex) Gaussian measurement errors (with possibly different variances for different k) which are uncorrelated across different k, and that the real and imaginary parts of w_k are also uncorrelated.

Note that in Section 3, we showed that $2n - 2$ (i.e. $N = 2n$ in 45) w-complex moments are necessary to uniquely recover the vertices of P. Here we allow the possibility that $N > 2n$ so that we may achieve some sensitivity reduction to errors in the $\hat{\tau}_k$. Collecting the measurements in (40) into vector form we have

$$
\begin{bmatrix} \hat{\tau}_0 \\ \hat{\tau}_1 \\ \vdots \\ \hat{\tau}_{N-1} \end{bmatrix} = \begin{bmatrix} 1 & 1 & \cdots & 1 \\ z_1 & z_2 & \cdots & z_n \\ \vdots & \vdots & \ddots & \vdots \\ z_1^{N-1} & z_2^{N-1} & \cdots & z_n^{N-1} \end{bmatrix} \begin{bmatrix} a_1 \\ a_2 \\ \vdots \\ a_n \end{bmatrix} + \begin{bmatrix} w_0 \\ w_1 \\ \vdots \\ w_{N-1} \end{bmatrix}
\tag{41}
$$

$$
\hat{T}_N = \mathcal{V}_N \mathbf{a}_n + W_N
\tag{42}
$$

Applying the $N \times N$ matrix K_N to both sides of (42) yields

$$
K_N \hat{T}_N = K_N W_N.
\tag{43}
$$

which can in turn be rewritten as

$$
\begin{bmatrix} \hat{\tau}_0 & \hat{\tau}_1 & \cdots & \hat{\tau}_{n-1} \\ \hat{\tau}_1 & \hat{\tau}_2 & \cdots & \hat{\tau}_n \\ \vdots & \vdots & \ddots & \vdots \\ \hat{\tau}_{N-n-1} & \hat{\tau}_{N-n} & \cdots & \hat{\tau}_{N-2} \end{bmatrix} p^{(n)} = - \begin{bmatrix} \hat{\tau}_n \\ \hat{\tau}_{n+1} \\ \vdots \\ \hat{\tau}_{N-1} \end{bmatrix}
\tag{44}
$$

$$
\hat{H}_N p^{(n)} = -\hat{h}_N
\tag{45}
$$

Equation (45) forms the basis of the Least Squares Prony technique. From this equation, the parameter

14

vector $\widehat{p}^{(n)}$ is estimated and subsequently, estimates of z_j are produced by solving the polynomial equation $\widehat{P}(z) = 0$, whose coefficients are the elements of $\widehat{p}^{(n)}$.

4.1.1 OLSP and WLSP

The Ordinary Least Squares Prony (OLSP) method consists of computing the least squares estimate of $p(n)$ from equation (45) by computing the generalized inverse of the matrix $\widehat{H}_N$ as follows.

$$\widehat{p}_{ols}^{(n)} = - \left(\widehat{H}_N^H \widehat{H}_N \right)^{-1} \widehat{H}_N^H \widehat{h}_N \tag{46}$$

where the superscript ^{H} denotes Hermitian transpose. With these estimated coefficients, the polynomial $\widehat{P}_{ols}(z) = 0$ is formed and factored to get OLSP estimates $\widehat{z}_j$ of the vertices. Having computed these estimates, we can form the matrix $\widehat{\mathcal{V}}_N$ as defined in (22), and then can estimate the vector $\mathbf{a}_n$ as

$$\widehat{\mathbf{a}}_n = \left(\widehat{\mathcal{V}}_N^H \widehat{\mathcal{V}}_N \right)^{-1} \widehat{\mathcal{V}}_N^H \widehat{\mathcal{T}}_N \tag{47}$$

The Weighted Least-Squares Prony (WLSP) solution can also be considered. In this formulation, the inverse of the covariance matrix for $\widehat{h}_N$ is used as a weighting factor. The resulting solution has the form

$$\widehat{p}_{wls}^{(n)} = - \left(\widehat{H}_N^H \Sigma \widehat{H}_N \right)^{-1} \widehat{H}_N^H \Sigma \widehat{h}_N \tag{48}$$

where Σ denotes the inverse of the covariance matrix for $\widehat{h}_N$.

4.1.2 TLSP

Equation (45) is an overdetermined system of linear equations of the form $Ax = b$ for the unknown $x = p^{(n)}$. The OLS procedure for estimating the desired parameters is appropriate when only the vector b is noisy. In fact, the OLS estimate coincides with the Maximum Likelihood (ML) estimate if the noise is taken to be Gaussian and white. In more general instances such as that of equation (45), both matrices A and b are corrupted by noise. For these cases, a more general fitting scheme called the Total Least Squares (TLS) has been devised [10, 15, 27] which can, in essence, be interpreted statistically as a regularized version of

the OLS solution. In particular, $\widehat{x}_{tls} = (A^H A - \sigma_{min}^2 I)^{-1} A^H b$, where σ_{min} denotes the minimum singular value of the concatenated matrix $[A, b]$. Applying this in our context, we find that the TLS estimate of $p^{(n)}$ is then given by

$$\widehat{p}_{tls}^{(n)} = -(\widehat{H}_N^H \widehat{H}_N - \sigma_{min}^2 I)^{-1} \widehat{H}_N^H \widehat{h}_N, \tag{49}$$

where σ_{min} is the smallest singular value of $[\widehat{H}_N, -\widehat{h}_N]$. Given this estimate, the TLS estimates for the vertices of the underlying n-gon are obtained as roots of the polynomial equation $\widehat{P}_{tls}(z) = 0$. Subsequently, TLS estimates of the vector $\mathbf{a}_N$ can be obtained as

$$\widehat{\mathbf{a}}_n = (\widehat{\mathcal{V}}_N^H \widehat{\mathcal{V}}_N - {\sigma'_{min}}^2 I)^{-1} \widehat{\mathcal{V}}_N^H \widehat{\mathcal{T}}_N, \tag{50}$$

where σ'_{min} is the smallest singular value of the matrix $[\widehat{\mathcal{V}}_N, \widehat{\mathcal{T}}_N]$.

5   An Application to Tomographic Reconstruction of Polygons

A novel application of the concepts and algorithms discussed above can be found in the field of tomographic reconstruction. By invoking a fundamental property of the Radon transform, we have shown [23, 20, 21] that the moments of an image can be recovered from its noisy projections. Hence, if the underlying image is assumed to consist of a simply-connected polygonal region, and a finite number of its (possibly noisy) projections are given, we can estimate the geometric (and hence complex) moments of the underlying polygon. If a sufficient number of these projections are available, then enough complex moments may be estimated to warrant a reconstruction of the underlying object via the algorithms discussed in this paper. To be more concrete, the Radon transform $g(t, \theta)$ of a square-integrable function $f(x, y)$ defined over a compact region of the plane $\mathcal{O}$ is given by

$$g(t, \theta) = \int \int_{\mathcal{O}} f(x, y) \delta(t - \omega \cdot [x, y]^T) dx dy, \tag{51}$$

where $\omega = [\cos(\theta), \sin(\theta)]$ and $\delta(\cdot)$ denotes the Dirac delta function. See Figure 2. The function $g(t, \theta)$

is square integrable [11] with finite support and is defined for each pair (t, θ) as the integral of f over a line at angle $\theta + \frac{\pi}{2}$ with the x-axis and at radial distance t away from the origin. An elementary result [11], which follows from the definition of the Radon transform, states that if $F(t)$ is *any* square integrable function, then the following relation holds true:

$$\int_{-T}^{T} g(t, \theta) F(t) dt = \int \int_{\mathcal{O}} f(x, y) F(\omega \cdot [x, y]^T) dx dy. \tag{52}$$

where T denotes the maximal support value of the set $\mathcal{O}$ in the direction θ defined by $T = \max_{\mathcal{O}}(x \cos(\theta) + y \sin(\theta))$. By considering $F(t) = e^{-it}$, the celebrated *Projection Slice Theorem* [12] is obtained. By letting $F(t) = t^k$ and expanding the right-hand side of (52) using the binomial theorem, we obtain

$$H^{(k)}(\theta) = \int_{-T}^{T} g(t, \theta) \, t^k \, dt = \sum_{j=0}^{k} \binom{k}{j} \cos^{k-j}(\theta) \, \sin^j(\theta) \, \mu_{k-j,j}. \tag{53}$$

which shows that the kth order geometric moment of the projection at angle θ is a linear combination of the kth order geometric moments of the image. Furthermore, we have proved the following [21, 23, 20]:

Proposition 3 *Given line integral projections of $f(x, y)$ at m different angles θ_j in $[0, \pi)$, one can uniquely determine the first m moment vectors $\mu^{(j)}$, $0 \le j < m$ of $f(x, y)$. This can be done using only the first m orthogonal moments $H^{(k)}(\theta_j)$, $0 \le k < m$ of the projections. Furthermore, moments of $f(x, y)$ of higher order cannot be uniquely determined from m projections.*

As a consequence of this result, and assuming projections corrupted by Gaussian white noise, it is a simple matter to compute ML estimates of the geometric moments of the image $f(x, y)$ from noisy measurements of its projections. In fact, this process is a straightforward *linear* estimation problem as outlined in [21, 23]. Once we have these estimates of the geometric moments of an image, the ML estimates of its complex moments are computed directly from (16). If the function $f(x, y)$ is taken to be the indicator function of a simply-connected polygon, what we have just described, along with the results and algorithms outlined in the earlier parts of this paper, allow the reconstruction of polygonal regions from a finite number of their

(noisy) Radon transform projections. In fact, it has long been of interest to know [16, 19, 17, 7, 8, 9] how many projections suffice to uniquely determine a simply-connected n-gon in the plane. To this end, we have the following corollary which follows directly from Propositions 3 and 1.

Corollary 3 *Exactly $2n - 2$ projections are sufficient to uniquely determine the vertices of a plane simply-connected polygonal region P.*

5.1 Numerical Examples

In this section we present some simulations to illustrate the reconstruction of polygonal objects from their noisy projections via moment estimation together with the application of standard array processing algorithms discussed in Section 4. In particular, we apply the least squares algorithms to the reconstruction of a triangle and a quadrilateral from ML estimates of w-complex moments obtained from projections. The prototypical triangle has been chosen as one with the following vertices

$$V = \begin{bmatrix} -0.4655 & 0.0082 & -0.3283 \\ 0.2201 & 0.4599 & -0.1809 \end{bmatrix} \tag{54}$$

The data $y(t_i, \theta_j) = g(t_i, \theta_j) + e_{ij}$ were collected in the form of $m = 20$ projections with $n = 500$ samples per projection at a signal-to-noise ratio of 23.9 dB, where the SNR is defined as follows:

$$\text{SNR} = 10 \log_{10} \frac{\sum_{i,j} g^2(t_i, \theta_j)/d}{\sigma^2}, \tag{55}$$

with $d = m \times n$ denoting the total number of samples of the function $g(t, \theta)$, and where σ^2 denotes the variance of the white noise sequence e_{ij}.

In all our simulations the reconstruction error is measured in terms of the percent Hausdorff distance [3] between the estimate and the true polygon. The Hausdorff metric is a proper notion of "distance" between two nonempty compact sets and it is defined as follows. Let $d(p^*, S)$ denote the minimum distance between the point p_1 and the compact set S: $d(p^*, S) = \inf\{\|p^* - p\| \mid p \in S\}$. Define the ϵ-*neighborhood* of the set

18

S as $S^{(\epsilon)} = \{p \mid d(p, S) \leq \epsilon\}$. Now given two non-empty compact sets, S_1 and S_2, the Hausdorff distance between them is defined as:

$$\mathcal{H}(S_1, S_2) = \inf\{\epsilon \mid S_1 \subset S_2^{(\epsilon)} \ and \ S_2 \subset S_1^{(\epsilon)}\} \tag{56}$$

In essence, the Hausdorff metric is a measure of the largest distance by which the sets S_1 and S_2 differ. The *percent* Hausdorff distance between the true object S and the reconstruction $\widehat{S}$ is now defined as

$$\text{Percent Error} = 100\% \times \frac{\mathcal{H}(\widehat{S}, S)}{\mathcal{H}(O, S)} \tag{57}$$

where O denotes the set composed of the single point at the origin, so that if S contains the origin, $\mathcal{H}(O, S)$ is the maximal distance of a point in the set to the origin and thus a measure of the set's size.

Figure 3 shows the performance curves for the three algorithms: Ordinary Least Squares Prony(OLSP), Total Least Squares Prony (TLSP), and Weighted Least Squares Prony (WLSP). These curves show average performance obtained by generating 100 runs of a Monte-Carlo simulation vs. the number of moments used over the minimum necessary (i.e. the overfit parameter). Recall that, according to Proposition 1, w-complex moments of up to order 5 are needed (at minimum) to reconstruct the triangle. Hence, an overfit parameter value of 2 corresponds to using estimated w-complex moments of up to order 7.

Note that overall, the TLSP algorithm performs best. The WLSP algorithm performs essentially the same for values of the overfit parameter larger than 2. This is due to the fact that as higher order moments are considered, these are weighed according to their inverse estimation error variances, and as shown in [21], the variance of the ML moment estimates obtained from projection data increases with moment order.

The graphs show that the overfit parameter value of 4 in the TLSP algorithm provides, on average, the best reconstructions. Note that the incorporation of even more moments does not improve the reconstruction error due to the fact that, because of the increasing uncertainty in the estimates of these moments, at some point their use results in diminishing returns.

Figures 4-7 show sample reconstructions for all the aforementioned algorithms for values 0, 2, 4, and 6 of the overfit parameter. An important point to note here is that while percent Hausdorff error is a useful metric for *comparing* different algorithms, as in Figure 3, an object and an estimate can have significant percent error difference while visually the estimate may appear nearly perfect (e.g. compare OLSP with an overfit of 2 in Figure 5 to the 10% error associated with it in Figure 3). Thus it is typically useful to display both performance curves as in Figure 3 *and* sample reconstructions as in Figures 4-7.

The quadrilateral to be reconstructed was chosen as the polygon P' shown in Figure 1. Projections from 20 equally spaced angles in $[0, \pi)$ were taken with 1000 samples per view at a signal to noise ratio of 65.2 dB. Reconstruction of the underlying polygon are shown with overfit parameter values of 0 in Figure 8. The corresponding estimated coefficients a'_j using OLS are: $a_1 = -0.0053 - 0.5868i$, $a_2 = -0.0308 + 1.0271i$, $a_3 = 0.4020 - 0.2422i$, $a_4 = -0.3659 - 0.1981i$, while the corresponding estimated coefficients using TLS and the actual values of these parameters can be seen in Table 1.

However, we are not yet finished, as we must decide on how the estimated vertices $\hat{z}_1$, $\hat{z}_2$, $\hat{z}_3$, and $\hat{z}_4$ should be connected. To decide how to do this, for either the TLSP or OLSP estimates, we use the estimated vertex locations in order to compute the coefficients a_j via formula (13) for each configuration, and compare these values to the corresponding estimated coefficients given above. The choice of configuration is then made according to which of the coefficient sets found using (13) most closely approximates the estimated coefficient set. Let us carry out this procedure for the TLS estimated vertices of the quadrilateral using overfit parameter of 0. For convenience, referring to Figure 1, we shall denote the configurations in which the vertices can be connected as P, P' and P'' respectively, so that the correct configuration is P'. The estimated coefficients using TLS, and the corresponding coefficients computed using (13) are shown in Table 1 along with the l^1 norm of their difference defined by:

$$l^1 \text{ Difference in } a_j\text{'s} = \sum_{j=1}^{4} \|a_j(\text{estimated}) - a_j(\text{from (13)})\|. \tag{58}$$

As can be seen from Table 1, as measured by the l^1 norm, the estimated coefficients are closest to the coefficients obtained when the estimated vertices are connected according to configuration P'. Hence, our algorithm has correctly identified the underlying configuration.

With an overfit parameter of 1, the reconstructions shown in Figure 9 are obtained. The corresponding values of the coefficients a_j are the same (to within 10^{-16}) as the previous case where an overfit parameter of 0 was used. The reconstructions using an overfit parameter of 2 are shown in Figure 10, where the estimated a_j parameters using OLS are: $a_1 = -0.0053 - 0.5868i$, $a_2 = -0.0308 + 1.0271i$, $a_3 = 0.4020 - 0.2422i$, $a_4 = -0.3659 - 0.1981i$. The estimates of these parameters using TLS are shown in Table 2.

Let us use these last set of estimated coefficients along with the estimated vertices using TLS, with overfit parameter of 2, to decide how the estimated vertices are to be connected. We again show the values of the coefficients obtained from (13) and the values of the total difference of these coefficients with the estimated coefficients in Table 2. In this case, the algorithm has again correctly chosen configuration P' as the solution, but note that the value of the l^1 difference of the coefficients for configurations P and P' are much closer than when an overfit parameter value of 0 was used. It is interesting to note that the use of higher order moments (i.e. overfit parameter > 0), which are noisier than the estimates of the lower order moments) worsens the estimate of the concave vertex of the underlying object more than the others.

6 Conclusion

In this paper we have presented algorithms for the reconstruction of binary polygonal shapes from noisy measurements of their moments. The mathematical basis of these algorithms is the Motzkin-Schoenberg

formula, and Prony's method. The contributions we have made in this paper can be grouped into two categories. From a mathematical standpoint, we have improved a result due to Davis which states that the vertices of a triangle are uniquely determined by its w- (or s-)complex moments of up to order 5 (or 3). Our generalization states that the vertices of any nondegenerate, simply-connected, n-sided polygon can be determined from its w- (or s-)complex moments up to order $2n - 1$ (or $2n - 3$). We have also shown that this number of moments is sufficient in some cases to uniquely specify the interior of the polygon.

From an estimation-theoretic viewpoint, we have established an explicit connection between the field of array signal processing and the problem of tomographic reconstruction of binary polygonal objects. We believe that the connection between tomographic reconstruction and array processing is a deep one, and the moment-based polygonal reconstruction represents one of several instantiations of that connection. Another such connection can be found in [1] in which an analogy is made between a straight line in an image and a planar propagating wavefront impinging on an array of sensors to obtain an array processing formulation for the detection of line parameters within an image, replacing the now classical Hough transform approach to the same problem. Still another can be seen directly from the geometry of the Radon transform. In particular, a well-known fact is that the set of points (t, θ) for which the value of $g(t, \theta)$ is influenced by the value of $f(x, y)$ at a given point, say (x_0, y_0), forms a sinusoid

$$t = x_0 \cos(\theta) + y_0 \sin(\theta) \tag{59}$$

and, in fact, for this reason a 2-D display of the Radon transform is known as a *sinogram*. Furthermore, one of the key steps in standard tomographic reconstruction, namely backprojection, simply corresponds to a type of beamforming or triangulation. For these reasons we believe that there is much yet to be done in exploiting the connections between tomography and array processing, and this paper represents one step in that direction.

On the other hand, it is equally important to point out that there are distinctive features of the tomog-

raphy problem that may lead to interesting adaptations and modifications of standard array processing techniques. In particular, while in this paper we demonstrate that standard array processing methods *can* be applied to the moment-to-polygon tomographic reconstruction problem, there are at least three significant differences between tomography and the array processing problem which we do *not* take advantage of here but which may lead to variations on array processing algorithms with enhanced performance for polygonal reconstruction.

The first we have already mentioned, namely the fact that the coefficients a_j in (40) are deterministic functions of the vertices z_1, z_2, $\cdots$, z_n, and the order in which they are connected. Making optimal use of this information would involve solving a highly nonlinear estimation problem. One suboptimal use of this relationship is illustrated in Section 5 in which we use the estimated a_j for each of several possible ways in which to connect the z_j in order to decide *which* of these ways is correct. Secondly, as we have discussed, in the tomographic problem if we have m projections, we can directly produce estimates of the full set of kth order geometric moments $\mu^{(k)}$ for each $k < m$ and not just the complex moment τ_k, which is a (complex) linear combination of the elements of $\mu^{(k)}$. Thus, in using only the τ_k in our reconstruction, we are not using all of the information extracted from the projections. While we do not pursue them here, there are at least two distinct ways in which the full set of tomographic information can be used in conjunction with the algorithms described here. First, we can use the $\mu^{(k)}$ in the process of deciding among the several possible ways to connect the estimated vertices, since the full set of *geometric* moments (rather than complex moments) do uniquely determine the polygon P. Alternatively in [22, 21] we describe iterative algorithms for tomographic reconstruction which require prior estimates of object support. For example in [22] we consider maximum likelihood estimation of the vertices directly from the original projection data. This is a highly nonconvex optimization problem requiring a good initial guess in order to work well. The method described here can provide such a guess. Finally, as we have noted and as is shown in [21, 23],

the error variances in the ML estimates of the moments $\hat{\tau}_k$ are a strong function of k, and in fact increase without bound as a function of the order of these moments [23]. This is in stark contrast to the constant variance assumption typically made for the sensor measurements in standard array processing problems [18, 14, 27, 25]. Hence, we may expect that the performance of the tomographic reconstruction algorithm described in this section may not be consistent with the performance of the corresponding algorithms when applied to a standard array processing scenario. Also, this suggests another line of further investigation in order to adapt standard methods to account for the variation in noise power found in moments estimated from tomographic data.

References

[1] Hamid K. Aghajan and Thomas Kailath. SLIDE: Subspace-based line detection. *To appear in the IEEE Trans. on PAMI*, 1994.

[2] O.B. Bekker, editor. *Spaces of Analytic Functions*, volume 512 of *Lecture Notes in Mathematics*. Springer-Verlag, 1975.

[3] Marcel Berger. *Geometry I and II*. Springer-Verlag, 1987.

[4] John B. Conway. *Function of One Complex Variable*. Graduate Texts in Mathematics. Springer Verlag, 2nd edition, 1978.

[5] P. J. Davis. Plane regions determined by complex moments. *Journal of Approximation Theory*, 19:148–153, 1977.

[6] Phillip J. Davis. Triangle formulas in the complex plane. *Mathematics of Computation*, 18:569–577, 1964.

[7] P. C. Fishburn, J. Lagarias, J. Reeds, and L. A. Shepp. Sets uniquely determined by projections on axes I. Continuous case. *SIAM J. Appl. Math.*, 50(1):288–306, 1990.

[8] R. Gardner. Sets determined by finitely many X-rays or projections. *Pubblicazzioni dell'istituto di analisi globale e applicazioni*, 50, 1990. Serie "Problemi non ben posti ed inversi".

[9] O. Giering. Bestimmung von eibereichen und einkorpern durch steiner-symmetrisierungen. *Sber. Bayer. Akad. Wiss. Munchen, Math. -Nat. Kl.*, pages 225–253, 1962.

[10] G.H. Golub and C.F. Van Loan. *Matrix Computations*. Johns Hopkins University Press, Baltimore, MD, 1983.

[11] Sigurdur Helgason. *Radon Transform*. Birkhauser, Boston, 1980.

[12] G. T. Hermann. *Image Reconstruction From Projections*. Academic Press, New York, 1980.

[13] A. Hildebrand. *Introduction to Numerical Analysis*. McGraw-Hill, New York, 1956.

[14] Yingbo Hua and Tapan Sarkar. Matrix pencil method for estimating parameters of exponentially damped/undamped sinusoids in noise. *IEEE Trans. on ASSP*, 38(5), May 1990.

[15] S. Van Huffel and J. Vandewalle. The use of total least squares techniques for identification and parameter estimation. In *Proc. 7th IFAC/IFORS Symp. on Identification and System Parameter Estimation*, pages 1167–1172, York, U.K., July 1985.

[16] A. Kuba. Reconstruction of measurable plane sets from their two projections taken in arbitrary directions. *Inverse Problems*, 7:101–107, 1991.

[17] A. Kuba and A. Volcic. Characterization of measurable plane sets which are reconstructable from their two projections. *Inverse Problems*, 4, 1988.

[18] R. Kumaresan and D.W. Tufts. Estimating the parameters of exponentially damped sinusoids and pole-zero modeling in noise. *IEEE Trans. on Acoust. Speech, Signal Processing*, ASSP-30:833–840, Dec. 1982.

[19] G.G. Lorentz. A problem of plane measure. *American Journal of Mathematics*, 71:417–426, 1949.

[20] P. Milanfar, W.C. Karl, and A.S. Willsky. Recovering the moments of a function from its Radon-transform projections: Necessary and sufficient conditions. LIDS Technical Report LIDS-P-2113, MIT, Laboratory for Information and Decision Systems, June 1992.

[21] P. Milanfar, W.C. Karl, and A.S. Willsky. A moment-based variational approach to tomographic reconstruction. *Submitted to: IEEE Transactions on Image Processing*, December 1993.

[22] P. Milanfar, W.C. Karl, and A.S. Willsky. Reconstructing finitely parameterized objects from projections: A statistical view. *Submitted to CVGIP: Graphical Models and Image Processing*, August 1993.

[23] Peyman Milanfar. *Geometric Estimation and Reconstruction from Tomographic Data*. PhD thesis, M.I.T., Department of Electrical Engineering, June 1993.

[24] H. Ouibrahim. Prony, Pisarenko, and the matrix pencil: A unified presentation. *IEEE Trans. ASSP*, 37(1):133–134, January 1989.

[25] R. Roy, A. Paulraj, and T. Kailath. ESPRIT: A subspace rotation approach to estimation of parameters of cissoids in noise. *IEEE Trans. ASSP*, ASSP-34(5):1340–1342, Oct 1986.

[26] Makato Sakai. A moment problem on Jordan domains. *Proceedings of the American Mathematical Society*, 70(1):35–38, June 1978.

[27] Louis L. Scharf. *Statistical Signal Processing*. Addison Wesley, 1991.

[28] R. O. Schmidt. *A signal subspace approach to multiple emitter location and spectral estimation*. PhD thesis, Stanford University, Stanford, CA, 1981.

[29] I.J. Schoenberg. *Approximation: Theory and Practice.* Stanford, CA, 1955. Notes by L.H. Lange on a series of lectures at Stanford University.

[30] V.N. Strakhov and M.A. Brodsky. On the uniqueness of the inverse logarithmic potential problem. *SIAM J. Appl. Math.*, 46(2):324–344, April 1986.

[31] L. Zalcman. *Integral Geometry*, volume 63 of *Contemporary Mathematics*, chapter Some Inverse Problems of Potential Theory, pages 337–350. American Mathematical Society, 1984.

Estimated a_j	a_j for P	a_j for P'	a_j for P''	Actual a_j
-0.0053-0.5872i	-0.1014 - 0.3998i	0.0155 - 0.6423i	0.1169 - 0.2424i	-0.6i
-0.0317 + 1.0539i	0.3837 - 0.4002i	0.2669 - 0.1577i	0.8735 + 0.2877i	i
0.4028 - 0.2463i	0.6066 + 0.4454i	0.1320 + 0.9875i	-0.4746 + 0.5421i	0.4-0.2i
-0.3664-0.2021i	-0.8890 + 0.3546i	-0.4144 - 0.1875i	-0.5158 - 0.5874i	-0.4-0.2i
l^1 Difference	3.2075	2.2601	3.1446	-

Table 1: Estimated, Computed, and Actual coefficients a_j for vertices of quadrilateral reconstructed using TLS with overfit parameter of 0

Estimated a_j	a_j for P	a_j for P'	a_j for P''
-0.0168-0.5774i	-0.0327 - 0.5684i	0.0452 - 0.6660i	0.0779 - 0.0976i
-0.0080 + 0.1809i	0.1250 - 0.1381i	0.0471 - 0.0405i	0.8478 + 0.3908i
0.4113- 0.1072i	0.8007 + 0.4313i	0.1092 + 0.8601i	-0.6915 + 0.4289i
-0.3997-0.0700i	-0.8930 + 0.2752i	-0.2015 - 0.1536i	-0.2342 - 0.7220i
l^1 Difference	1.6305	1.5648	3.2691

Table 2: Estimated and Computed coefficients a_j for vertices of quadrilateral reconstructed using TLS with overfit parameter of 2
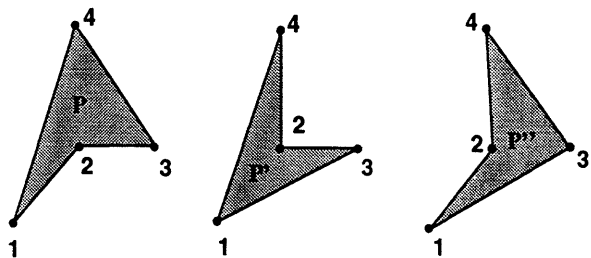
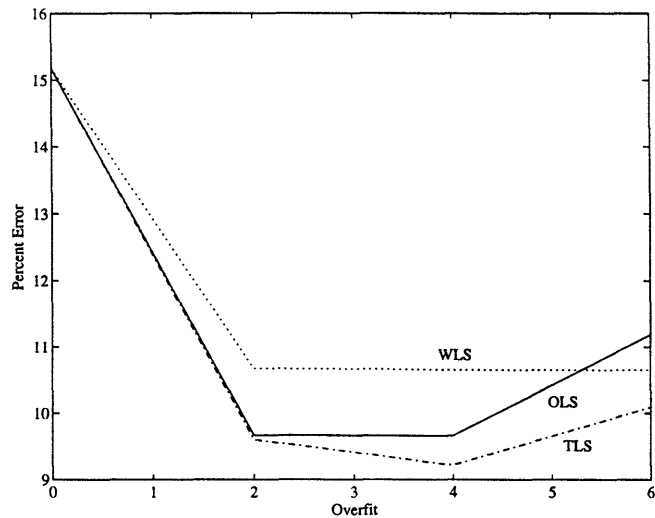Figure 1: Three distinct regions corresponding to the same vertices

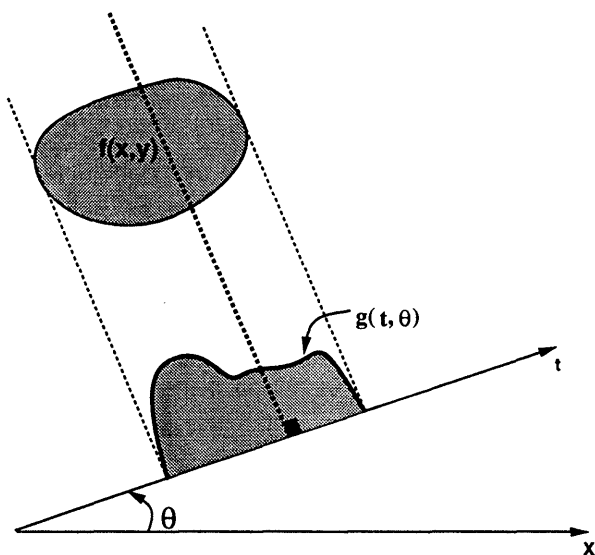

Figure 3: Overlayed performance curves at SNR=23.9 dB
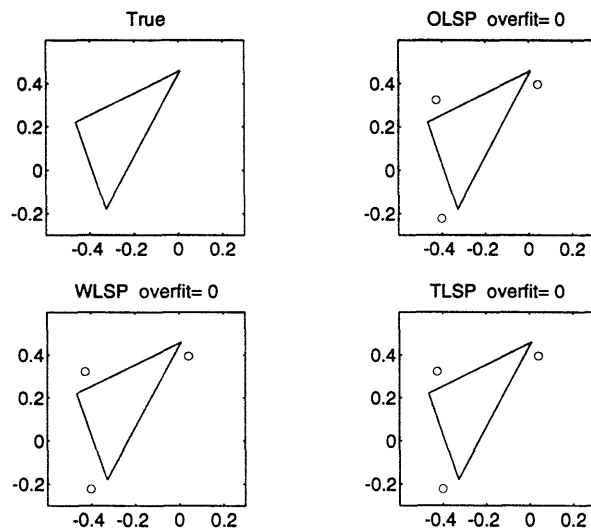

Figure 2: The Radon transform

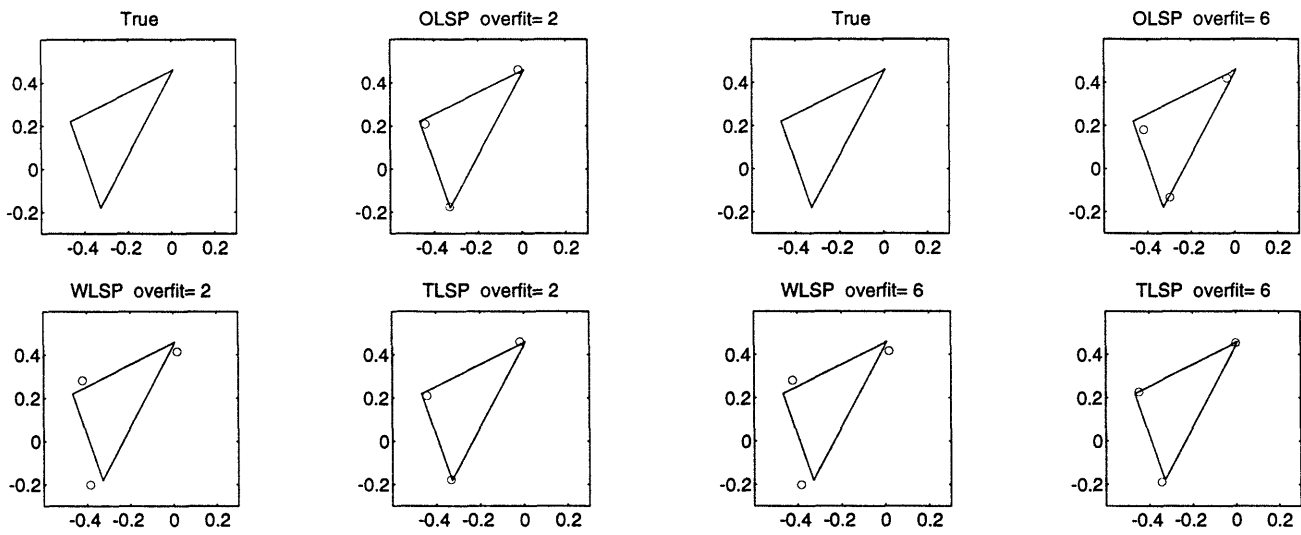Figure 4: Sample reconstructions at SNR=23.9 dB solid: actual, cirles: reconstructed

28

Figure 5: Sample reconstructions at SNR=23.9 dB
solid: actual, cirles: reconstructed

Figure 7: Sample reconstructions at SNR=23.9 dB
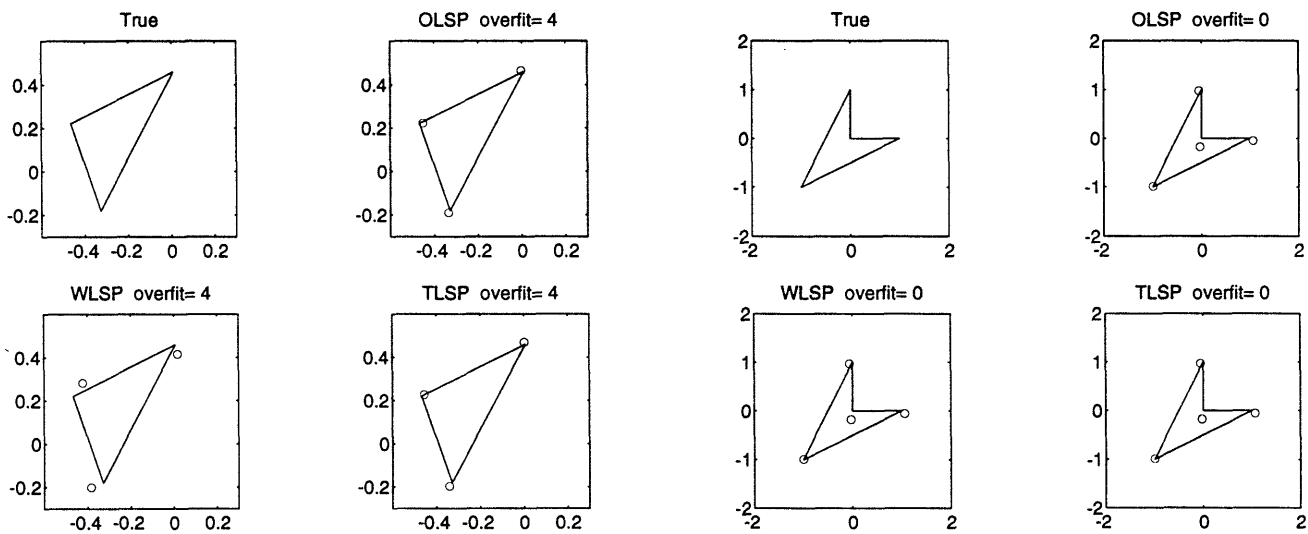solid: actual, cirles: reconstructed

Figure 6: Sample reconstructions at SNR=23.9 dB
solid: actual, cirles: reconstructed

Figure 8: Sample reconstructions at SNR=65.2 dB
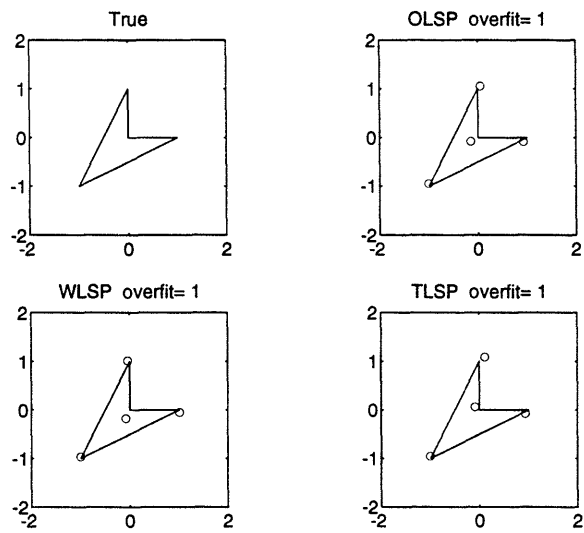solid: actual, circles: reconstructions

Figure 9: Sample reconstructions at SNR=65.2 dB solid: actual, circles: reconstructions
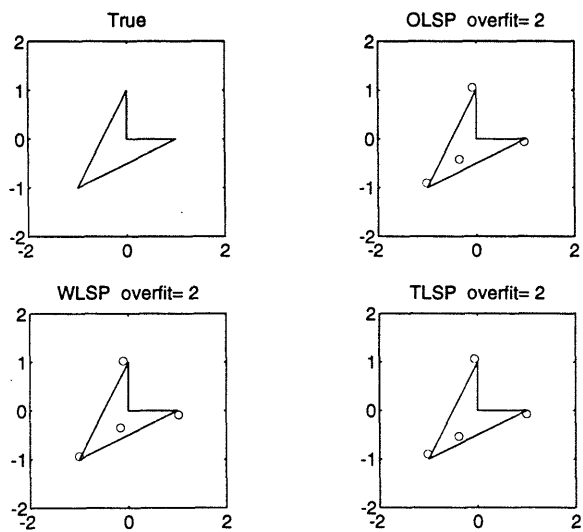

Figure 10: Sample reconstructions at SNR=65.2 dB solid: actual, circles: reconstructions